



An investigation on the effects of nanoplastic particles on *Chlorella vulgaris* enzymes and its function on removal of nitrate and phosphate

Maryamsadat Shahidi^a, Parichehr Hanachi^{a*}, Mehdi Khoshnamvand^a
Masoomeh Shafieia^a and Hamieh Goshtasbi^b

Article DOI:

[10.55434/CBI.2023.20102](https://doi.org/10.55434/CBI.2023.20102)

Author's Affiliations

^aDepartment of Biotechnology, Faculty of Biological Sciences, Alzahra University, Tehran, Iran

Department of Plant, Cell and Molecular Biology, Faculty of Natural Sciences, University of Tabriz, Tabriz, Iran

Corresponding Authors

Parichehr Hanachi

p.hanachi@alzahra.ac.ir

Received- 13-12-2023,

Accepted- 31-12-2023

©2023 The Authors Published under
Caribbean Journal of Science and
Technology

ISSN 0799-3757

<http://caribjcsitech.com/>

Abstract

Plastic waste at sea has been a primary environmental concern for years. The degradation of plastics into small pieces leads to the formation of nanoplastics (NPs) (less than 100 nm) that can enter the environment. Polystyrene is one of the most common plastics, a product of the polymerization of styrene monomers. In this study, the toxic effects of amino polystyrene (PS-NH₂) NPs with sizes 90 (PS-NH₂-90), 200 (PS-NH₂-200), and 300 (PS-NH₂-300) nm with four different concentrations after 72 hours on viability, activity of enzymes such as superoxide dismutase (SOD), catalase (CAT), glutathione S-Transferase (GST) and reduced glutathione (GSH), carbonyl protein and sulfhydryl protein and antioxidant activity assay by DPPH reagent on the *Chlorella vulgaris* were investigated. In all enzymatic assays, except the glutathione (GSH) and sulfhydryl protein, the size of 90 nm showed lowest value. Intriguingly, flow cytometry assessment showed a substantial reduction in the viability at PS-NH₂-90 treated samples for 72 h which means that as the size of the nanoplastic decreases, its toxicity will increase. The toxicity effect of 90 nm NPs with a concentration of 200 mg/L on the microalgae *C. vulgaris* (with a concentration of 25000 Cells/mL) with the aim of bioremediation of nitrate (with a concentration of 50 mg/L) and phosphate (with a concentration of 6 mg/L) were investigated. According to the obtained results, NPs with a concentration of 200 mg/L with a size of 90 nm have the highest toxicity on the nitrate and phosphate bioremediation by the *C vulgaris* with a concentration of 25000 Cells/mL.

Keywords

Amino polystyrene nanoplastics (PS-NH₂); *Chlorella vulgaris*; Enzyme activity; Nitrate and Phosphate removal; Plastic contamination.

Introduction

Worldwide, plastic use is growing year by year, with current figures showing plastic production exceeding 368 million tons in 2019. Once disposed of, plastic waste is exposed to biological, chemical and environmental elements, and will break down into huge amounts of microplastics (measuring < 5 mm) and nanoplastics (NPs) (<0.1 μm). Pollution from plastic waste has been a growing problem since the mass production of plastics in the 1940 s. As this is a potential threat to terrestrial and aquatic ecosystems, pollution from these plastics has become a severe global crisis. Polystyrene is a plastic with wide applications in many industries and human life due to its useful features such as low cost, lightness, ease of production, versatility and moisture resistance.

This polymer is very stable and resistant to decomposition in nature. NP and its potential effects on viability, development, and reproduction of organisms through potential mechanisms, such as stimulation, disruption of damaged tissues, and disruption of fatty acid metabolism.¹⁻⁷

NPs are more deadly than microplastics because they can be easily consumed by marine organisms. They pass through cell membranes that act as a barrier against foreign matter, penetrate tissues, and accumulate in organs. NPs can interact with the biological system of living organisms when they cross barriers. These particles can act as carriers of environmental chemical pollutants and pesticides. Absorption of these particles by living organisms, especially aquatic organisms, may cause changes in gene expression as well as the activity of enzymes in the antioxidant pathway⁶. Toxicity studies using NPs on marine organisms have increased in recent years using carboxylic (PS-COOH) and amino (PS-NH₂) polystyrene as model particles. It is well established that microalgae communities play an essential role in aquatic ecosystems because they are the primary producers of food chain consumers and also oxygen producers^{1, 8}. Therefore, these organisms are the most important models for studying the aquatic system. *C. vulgaris* is a freshwater single-celled microalgae, spherical and 2 to 10 μm in diameter, which plays a vital role in the ecosystem. The algae reproduce rapidly within 24 hours under optimal conditions. Therefore, it is widely used as an aquatic organism to study the toxic effects of pollutants^{9,10}. Since reports of size-dependent toxicity of amino polystyrene nanoplastic (PS-NH₂) on the enzymatic activity of *C. vulgaris* microalgae have been limited, in this study, the most toxic of amino polystyrene nanoplastic size (PS-NH₂) is, smallest one such as in 90nm on protein and enzymatic activity of *C. vulgaris* microalgae. Also, the study of images obtained by light microscopy and FESEM showed that high concentrations of PS-NH₂ can produce PS-NH₂ clumps and algae that can change the bioavailability, mobility, fate, and toxicity of PS-NH₂¹⁰. The results of this study can help to understand the ecological problems caused by the toxicity of amino polystyrene nanoplastic (PS-NH₂) in environments containing these nanoparticles.

Materials and Methods

Preparation of polystyrene nanoplastics coated with amine functional groups (PS-NH₂)

Polystyrene NPs coated with amine functional groups (PS-NH₂) with positive electric charge (to prevent aggregation) in sizes of 90, 200, and 300 nm for colloidal and water-soluble experiments from Tianjin Saierqun Technology Company of China were purchased (Tianjin, China [http://www.tjseq.com]). *C. vulgaris* microalgae were prepared from the Iranian National Algae Culture Collection (INACC, University of Tehran, Tehran, Iran).

Cultivation of *Chlorella vulgaris*

Algal cells in 1-liter Erlenmeyer at temperatures between 30-32 °C, under continuous fluorescent light with continuous aeration by oxygen pump and pH 7.5 in the standard culture medium suggested by the Organization for Economic Cooperation and Development, OECD Guideline No. 201, were grown (OECD, 2011). This medium contains amounts of macronutrients (NH₄Cl, MgCl₂·6H₂O, CaCl₂·2H₂O, MgSO₄·7H₂O, KH₂PO₄), iron (FeCl₃·6H₂O, Na₂EDTA 2H₂O), trace elements (H₃BO₃, MnCl₂·4H₂O, ZnCl₂, CoCl₂·6H₂O, CuCl₂·2H₂O, Na₂MoO₄·2H₂O) and bicarbonate (NaHCO₃, Na₂SiO₃·9H₂O) were required for the growth of algal cells.

Toxicity Assays

When algal cultures reached the exponential growth phase, they were used for toxicity tests. Toxicity tests were performed using PS-NH₂ (90, 200, and 300 nm) in 4 different and incremental concentrations (25, 50, 100, and 200 mg/l) and their effects on enzyme activity and oxidative stress. 250 ml of *C. vulgaris* microalgae with an initial density of 2.5×10⁴ cells/ml were used to survey the short-term effects of these treatments. The toxicity effect of different concentrations of PS-NH₂ (90, 200, and 300 nm) was assessed on enzyme activity and oxidative stress of *C. vulgaris* after 72 h. Three replicates were evaluated for each experiment.

Superoxide Dismutase (SOD) Activity Assay

The superoxide dismutase activity was determined by measuring the inhibition of nitroblue tetrazolium in photoreduction (NBT) at 560 nm. The enzyme activity study experiments were performed at room temperature and the amount of enzyme activity was calculated using the following formula¹¹.

$$\text{SOD inhibition ratio} = \frac{\text{OD}_{\text{Control}} - \text{OD}_{\text{Sample}}}{\text{OD}_{\text{Control}}} \times 100$$

SOD activity (U/mg) = SOD inhibition ratio/ %50× reaction solution dilution ratio/ total protein concentration.

Catalase Activity Assay

Catalase activity following the reduction of hydrogen peroxide (H₂O₂) absorption with an extinction coefficient of 43.6 M⁻¹.Cm⁻¹ was measured for 2 minutes at a wavelength of 240 nm¹². Adsorption was recorded with the ELISA reader at 240 nm for 2 min.

Glutathione-S-Transferase (GST) Assay

Glutathione s-transferase catalyzes the conjugation reaction or binding of xenobiotic compounds to the thiol group of reduced glutathione. 1-Chloro-4-2-dinitrobenzene (CDNB) and glutathione were used as enzyme substrates. During the reaction, the CDNB was converted to a dye called nitrophenyl thioester, which was adsorbed at 340 nm. Enzyme activity was calculated by measuring the adsorption of this dye at 340 nm¹³. The adsorption of the final solution was read twice at 5-minute intervals by the ELISA reader, then the activity of the GST enzyme using an extinction coefficient of 9.6 M⁻¹. Cm⁻¹ was calculated for the composition (glutathione + CDNB) using the following formula. The path length in ELISA wells is 0.524 cm, which is multiplied by the extinction coefficient, and the result was 0.00503 in the formula.

$$GST \text{ Activity (min/ mg)} = (\Delta A / \Delta t) / 0.00503 \times vt / ve \times 1 / P \times F_d$$

Reduced Glutathione (GSH) Assay

Glutathione sulfhydryl (SH) groups react with Ellman reagent or 5,5'-dithio-bis-[2-nitrobenzoic acid] (DTNB) to produce a yellow substance called TNB. GSTNB disulfide produced during the previous reaction can be regenerated by glutathione reductase to produce GSH and TNB. Therefore, by measuring the concentration of TNB at a wavelength of 412 nm, the concentration of glutathione can be calculated¹⁴. The optical absorption of the samples and blanks was read at 412 nm, and the concentration of the samples was calculated according to the formula of Beer Lambert's law. The extinction coefficient of TNB is 13.6 mM⁻¹.Cm⁻¹.

$$A = \epsilon.L.C$$

Protein Carbonyl Assay

Reactions between 2,4-dinitrophenyl-hydrazine (DNPH) and carbonyl protein were used to determine the carbonyl content of the protein. After reacting with the carbonyl protein to form a

Schiff base, DNPH produces a hydrazone derivative with maximum absorption at 370 nm¹⁵.

Protein Sulfhydryl Assay

The reaction between sulfhydryl protein groups with Ellman reagent or 5,5'-dithiobis (2-nitrobenzoic acid (DTNB) was used. DTNB is an aromatic disulfide with a higher standard oxidation-reduction potential than aliphatic analogs. The Ellman reagent performs a substitution reaction with aliphatic thiols, resulting in one mole of protein-attached disulfide and one mole of 2-nitro-5-thiobenzoate anion per sulfhydryl protein group. The reaction between the disulfide groups of the reagent and the thiol groups of the protein can continue. For each mole of sulfhydryl protein, one mole of 2-nitro-5-thiobenzoate is produced, which is yellow and has a maximum absorption at 410 nm¹⁶. If the optical absorption of the sample, sample blank, and reagent blank is called OD₁, OD₂, and OD₃, respectively, the calculations for the sulfhydryl protein groups were determined by the following method, and the concentration of the samples was determined by the formula of Beer Lambert's law. The extinction coefficient is 13600 M⁻¹Cm⁻¹.

$$A = OD_1 - OD_2 - OD_3$$

$$A = \epsilon.L.C$$

Antioxidant Activity Assay by DPPH Reagent

2,2-diphenyl-1-picrylhydrazyl or DPPH are stable free radicals with electrons unpaired in their capacitance layer. It has the highest absorption at 517 nm. This radical is purple in solution. The antioxidants that give electrons change from DPPH, and the color of the solution changes from purple to yellow. The greater the color change the lower the absorption at 517 nm¹⁷.

Nitrate

For samples and standards, subtract two times the absorbance reading at 275 nm from the reading at 220 nm to obtain absorbance due to NO₃⁻-N. If the correction value is 10% of reading at 220 nm for a particular sample, then the NO₃⁻-N concentration is considered a rough estimate. Use an electronic spreadsheet, a calculator, or instrument software to find the slope and intercept of the calibration curve by least squares linear regression. Calculate the NO₃⁻-N concentration from the following equation¹⁸.

$$C = (A - I) / S$$

C = concentration,

A = absorbance,

I = intercept of the regression line, and

S = slope of the regression line

Phosphate

Set the spectrophotometer at 625 nm in the measurement of benzene-isobutanol extracts and at 690 nm for aqueous solutions. Measure color photometrically at 690 nm and compare with a calibration curve, using a distilled water blank¹⁸.

Statistical analysis

Data were expressed as mean ± standard deviation (SD ±) and for normal distribution and homogeneity of variances using Shapiro-Wilk and Levene's methods. SPSS software version 26.0 (SPSS Inc., Chicago, IL, USA) was used for data analysis. Statistical differences between samples were determined using one-way analysis of variance (ANOVA) at the significant level of p < 0.05 and post-hoc Duncan's test. Microsoft Excel version 2013 (Microsoft Corporation, Redmond, WA, USA) was used for graphic outputs.

Results

PS-NH₂ characterization

A field emission scanning electron microscope (FESEM) was applied to display structure and size of PS-NH₂. FESEM images confirmed that PS-NH₂ used in this study with different diameters (i.e., 90, 200, and 300 nm) were spherical (Fig. 1A–C). PS-NH₂ suspensions appeared colorless and clear with no precipitates. Positive charges of PS-NH₂ prevented them from aggregation and allowed them to remain in suspension in the colloidal solution (Fig. 1).

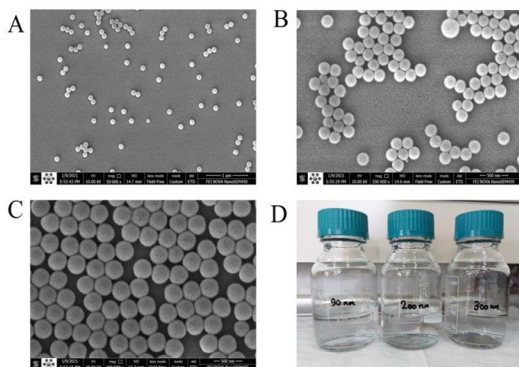


Figure 1: FESEM images of PS-NH₂ with diameters of (A) 90, (B) 200, and (C) 300 nm. (D) Suspensions of PS-NH₂ were used in this study with various diameters.

Superoxide Dismutase Assay (SOD)

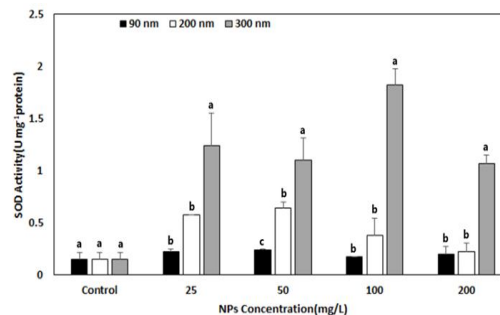


Fig. 2: Polystyrene NPs coated with amine functional groups (PS-NH₂) Toxicity in different treatments on SOD activity. Data are expressed as mean ± standard deviation. Columns labeled with different letters are significantly different (p ≤ 0.05).

The Fig. 2 showed the effect of PS-NH₂ toxicity in three different sizes on SOD enzyme activity. The results showed that the enzyme activity in the treatment with three sizes of 90, 200, and 300 nm increased compared to the control. It was also found that by reducing the size of PS-NH₂ and increasing its concentration, the toxicity of PS-NH₂ on *C. vulgaris* was intensified. The lowest to highest toxicity was observed at concentrations of 25, 50, 100, and 200 mg/l PS-NH₂, respectively.

Catalase

The results showed that the catalase activity in various concentrations and sizes of PS-NH₂ increased compared to the control (Fig. 3). In the treated samples, PS-NH₂ with a size of 90 nm had the lowest activity and therefore the highest toxicity in all concentrations of 25, 50, 100, and 200 mg/L. In the treatment with a size of 300 nm at concentrations of 25, 50, and 200 mg/L, compared to the size of 200 nm, the activity of CAT was less. However, in the treatment with a size of 300 nm at a concentration of 100 mg/L, the activity of CAT was higher than the size of 200 nm.

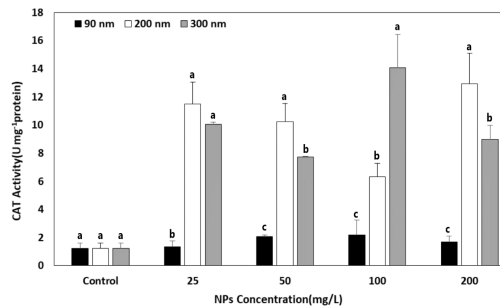


Fig. 3: Polystyrene NPs coated with amine functional groups (PS-NH₂) Toxicity in different treatments on CAT activity. Data are expressed as mean ± standard deviation. Columns labeled with different letters are significantly different (p ≤ 0.05).

This indicates more toxicity of PS-NH₂ with a size of 300 nm at concentrations of 25, 50, and 200 mg/L than the size of 200 nm. In contrast, about a concentration of 100 mg/L, the toxicity of PS-NH₂ with a size of 200 is greater than the size of 300 nm.

Glutathione S-Transferase(GST)

PS-NH₂ with a size of 90 nm in all concentrations of 25, 50, 100, and 200 mg/l had no significant effect on GST enzyme activity compared to the control subsequently the most toxicity is in this size (Fig. 4). The activity of GST enzyme in the treatment with a size of 300 nm at concentrations of 50, 100, and 200 mg/L compared to the size of 200 nm, was lower, but in the treatment with a size of 300 nm at a concentration of 25 mg/l nanoplastic compared to the size of 200 nm the decrease in GST enzyme activity was minor. At concentrations of 25, 50, and 100 mg/l, all three dimensions have significant differences, while at concentrations of 200 mg/l, sizes 90 and 300 have substantial differences with a size of 200 nm.

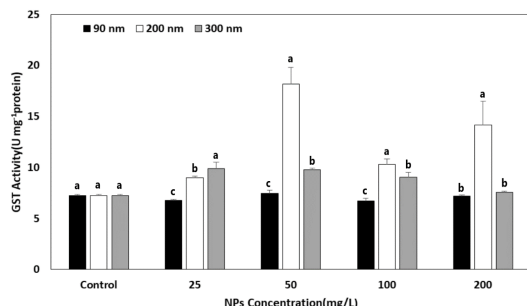


Fig. 4: Polystyrene NPs coated with amine functional groups (PS-NH₂) Toxicity in different treatments on GST enzyme activity. Data are expressed as mean ± standard deviation. Columns labeled with different letters are significantly different (p ≤ 0.05).

Glutathione (GSH)

Results showed that the activity of GSH in the treatment with a size of 200 nm increased at all concentrations of 25, 50, 100, and 200 mg/l NPs (Fig. 5). Samples treatment with concentrations of 25 and 50 mg/l of 90 nm NPs caused more GSH activity than 300 nm nanoparticles. However, in the treatment of the samples with 90 nm NPs, at concentrations of 100 and 200 mg/l, a decrease in activity was observed compared to 300 nm particles .This indicates the more significant toxicity of nanoplastic with a size of 90 nm at concentrations of 100 and 200 mg/l compared to the size of 300 nm, while at a concentration of 25 and 50 mg/l, the toxicity of nanoplastic with a size of 300 is greater than the size of 90 nm. At a concentration of 25 mg/l, all three sizes are

significantly different. At concentrations of 50, 100, and 200 mg/l, sizes 90 and 300, there is a significant difference with a size of 200 nm.

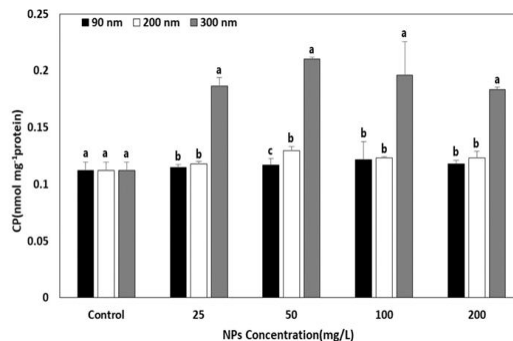


Fig. 5: Polystyrene NPs coated with amine functional groups (PS-NH₂) toxicity in different treatments on GSH activity. Data are expressed as mean ± standard deviation. Columns labeled with different letters are significantly different (P ≤ 0.05).

Protein Carbonyl

Carbonyl groups of producers are considered another indicator of a critical stress state. Carbonyl groups are naturally present in the diet. The attack of free radicals on cells increases the amino acids and creates carbonyl groups that affect tperformance of the cell. Fig. 6 showed the effect of nanoplastic toxicity in three different sizes on the amount of carbonyl protein.

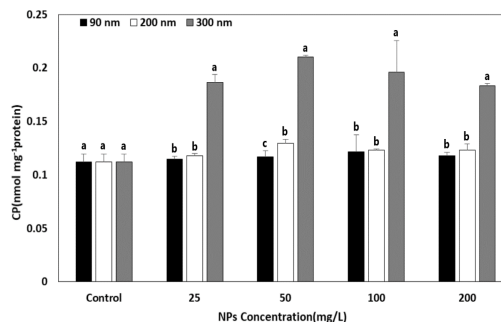


Fig. 6: Graph of toxicity of polystyrene NPs coated with amine functional groups (PS-NH₂) in different treatments on carbonyl protein content. Data are expressed as mean ± standard deviation. Columns labeled with different letters are significantly different (p ≤ 0.05).

Based on the results, the lower the amount of carbonyl protein showed in smaller the microplastic. Moreover, results showed that the amount of carbonyl protein in the treatment with three sizes of 90, 200, and 300 nm has the highest to lowest toxicity at all concentrations of 25, 50, 100, and 200 mg/l nanoplastic. At a concentration of 50 mg/l, all three sizes are significantly different from each other. At concentrations of 25, 100, and

200 mg/l, sizes 90 and 200, there is a significant difference with a size of 300 nm.

Protein sulfhydryl

The amount of sulfhydryl protein in the treatment with three sizes of 90, 200, and 300 nm PS-NH₂ decreased with increasing size and increasing concentration. According to the results, with decreasing the size of nanoplastic, the amount of sulfhydryl protein in *C. vulgaris* has increased, and the lowest amount of sulfhydryl protein has been observed in the sample treated with nanoplastic with a size of 300 nm (Fig. 7).

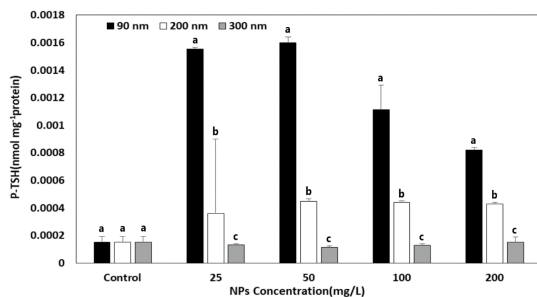


Fig. 7: Polystyrene NPs coated with amine functional groups (PS-NH₂) toxicity in different treatments on sulfhydryl protein content. Data are expressed as mean ± standard deviation. Columns labeled with different letters are significantly different (p ≤ 0.05).

DPPH

The antioxidant activity in the treatment with three sizes of 90, 200, and 300 nm compared to the control samples, except for the concentration of 50 mg/l nanoplastic in the size of 200 nm, was reduced (Fig. 8). Also, by reducing the size of nanoplastic and increasing its concentration, the toxicity of nanoparticles on *C. vulgaris* has intensified. At 90 nm size, the lowest to highest toxicity was observed at concentrations of 25, 50, 100, and 200 mg/l nanoplastic, respectively. In the treatment with a size of 200 nm in 25, 100, and 200 mg/l and the treatment with a size of 300 nm in 25 and 100 mg/l nanoplastic, the amount of antioxidant activity is reduced, and in the treatment with a size of 300 nm in the concentrations of 50 and 200 mg/l nanoplastic did not change. According to the diagram, it can be concluded that 90 nm nanoplastic is more toxic at concentrations of 50, 100, and 200 mg/l than the sizes of 200 and 300 nm.

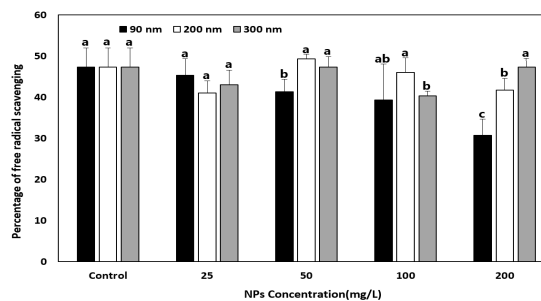


Fig. 8: Polystyrene NPs coated with amine functional groups (PS-NH₂) Toxicity in different treatments on antioxidant activity. Data are expressed as mean ± standard deviation. Columns labeled with different letters are significantly different (p ≤ 0.05).

Flow cytometry

To estimate of viability of the algal cells, *C. vulgaris* treated with PS-NH₂ using Annexin v, PI was removed due to its spectrum overlap (620 nm) with photosynthetic pigments spectrum in *C. vulgaris* (600-700 nm). The viability of the control sample was almost 100% (Fig. 9A). In comparison with the control samples, after 72 h, 74.64%, 59.15%, and 52.91% decline in cell viability were observed in the treatment with three sizes of 90, 200, and 300 nm when cells were exposed to 100 mg L⁻¹ of PS-NH₂ (Fig. 9A, C, and E).

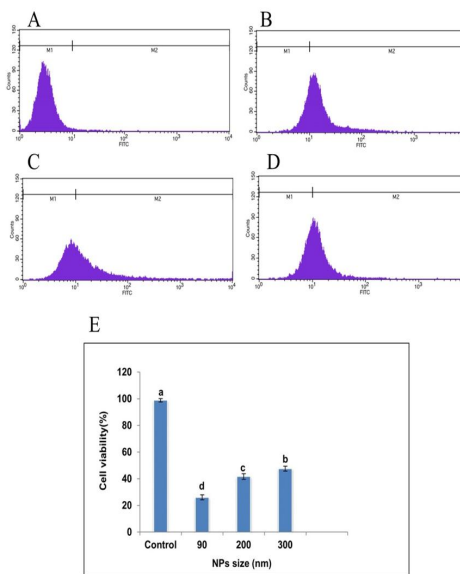


Fig. 9: Flow cytometry images. A: A control sample of *C. vulgaris* showed nearly 100% cell viability after 24 h. B, C, and D: Cell viability of *C. vulgaris* after 72-h treatment with 200 mg L⁻¹ (PS-NH₂) with three sizes of 90, 200, and 300 nm respectively. Data are expressed as mean ± standard deviation. Columns labeled with different letters are significantly different (p ≤ 0.05).

First week; nitrate

At the end of 144 hours and after 6 days, the amount of nitrate in the concentration of 50,000 Cells/mL, and at the end of 192 hours, with the passage of 8 days, the amount of nitrate in the concentration of 12,500 Cells/mL of *C. vulgaris* microalgae with a significant difference ($p \leq 0.05$) have had the most reductions (Fig. 10). By examining the control sample, which is displayed in white, it can be concluded that, except for 192 hours, there was no significant difference ($p \leq 0.05$) with other groups on all days of measurement. By examining the 6250 Cells/mL sample which is displayed in black, it can be concluded that in 192 hours, it had the highest nitrate reduction in all the days of measurement compared to other groups. By examining the 12500 Cells/mL sample which is displayed in gray, it can be concluded that all four-time groups had a significant difference ($p \leq 0.05$) with each other in such a way that 96 and 192 hours have had the lowest and highest decrease respectively. By examining the 25000 Cells/mL sample which is displayed with stripes, it can be concluded that there was a significant difference ($p \leq 0.05$) with other groups at 48 and 96 hours, and the lowest decrease is related to 192. By examining the 50,000 Cells/mL sample, which is displayed with a dotted, it can be concluded that all groups have a significant difference ($p < 0.05$) and the more time has passed, the nitrate level has decreased.

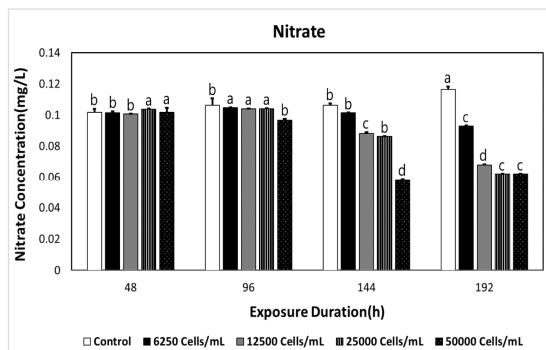


Fig. 10: Biomass of microalgae *C. vulgaris* in the presence of the same concentration of nitrate. Lowercase letters indicate significant differences between groups ($p \leq 0.05$). The white, black, gray, striped, and dotted charts indicate the number of algae cells 0, 25000, 12500, 6250, and 50000, respectively.

First week; phosphate

At the end of 144 hours after 6 days at a concentration of 50000 Cells/mL and at the end of 192 hours after 8 days, the amount of phosphate at concentrations of 6250 and 12500 Cells/mL of *C. vulgaris* microalgae with a significant difference ($p \leq 0.05$) have had the highest reductions (Fig. 11). By examining the control sample which is displayed in white, it can be concluded that it has a significant difference ($p < 0.05$) with other groups at

96 and 192 hours, and the highest phosphate reduction is related to 144 hours. By examining the samples of 6250 and 12500 cells/mL, which are shown in black and gray respectively, all groups have a significant difference ($p < 0.05$) and the more time has passed, the amount of phosphate has decreased. By examining the 25000 Cells/mL sample which is displayed with stripes, it can be concluded that there was a significant difference with other groups in 96 and 144, and also the lowest amount of phosphate is related to these two groups. By examining the 50000 Cells/mL which is displayed with a dotted, it can be concluded that all groups have a significant difference ($p < 0.05$), and the lowest reduction is related to the 144 hour group.

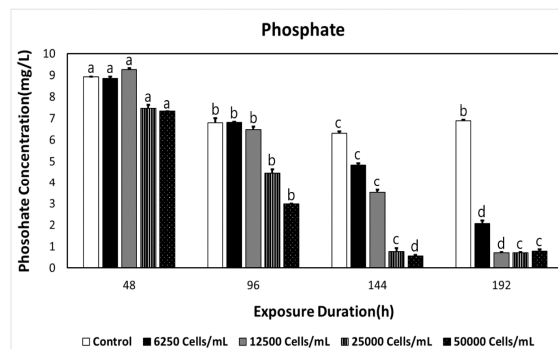


Fig. 11: Biomass of microalgae *C. vulgaris* in the presence of the same concentration of phosphate. Lowercase letters indicate significant differences between groups ($p \leq 0.05$). The white, black, gray, striped, and dotted charts indicate the number of algae cells 0, 25000, 12500, 6250, and 50000, respectively.

Second week; biomass

In all nanoplastic concentrations and over time, the biomass of *C. vulgaris* microalgae is increasing with a significant difference ($p < 0.05$) (Fig. 12).

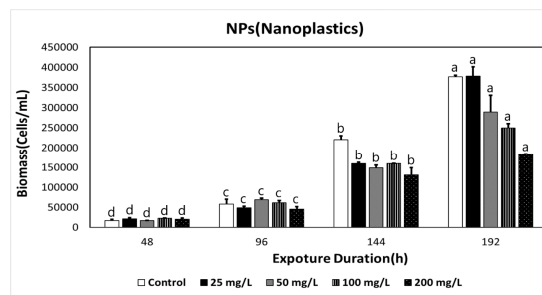


Fig. 12: Biomass of *C. vulgaris* microalgae. Lowercase letters indicate significant differences between groups ($p \leq 0.05$). The white, black, gray, striped, and dotted charts indicate nanoplastic concentrations of 0, 100, 50, 25 and 200 mg/liter, respectively.

Third week; nitrate

At the end of 192 hours and 8 days later, the amount of nitrate in the concentration of 200 mg/L of nanoplastic decreased the most with a significant difference ($p \leq 0.05$) (Fig. 13). By examining the control samples, 25, 50, 100, and 200 mg/L NPs, which are displayed with white, black, gray, striped, and dotted, respectively, it can be concluded that there is a significant difference ($p < 0.05$) in all hours and over time the amount of nitrate is decreasing.

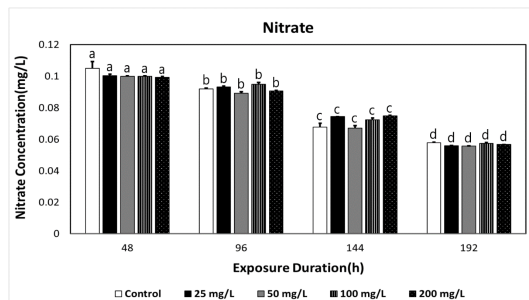


Fig. 13: Microalgae biomass of *C. vulgaris* in the presence of the same concentration of nitrate and microplastic. Lowercase letters indicate significant differences between groups ($p \leq 0.05$). The white, black, gray, striped, and dotted charts indicate nanoplastic concentrations of 0, 100, 50, 25, and 200 mg/L, respectively

Third week; phosphate

At the end of 144 hours and 6 days later, the amount of phosphate in the concentration of 200 mg/L of nanoplastic has decreased the most with a significant difference ($p \leq 0.05$) (Fig. 14). By examining the control, 25 and 50 mg/L of NPs, which are displayed in white, black, and gray, respectively, it can be concluded that the groups of 144 and 192 hours have a significant difference ($p < 0.05$) with the groups of 96 and 48 hours and over time, the amount of phosphate is decreasing.

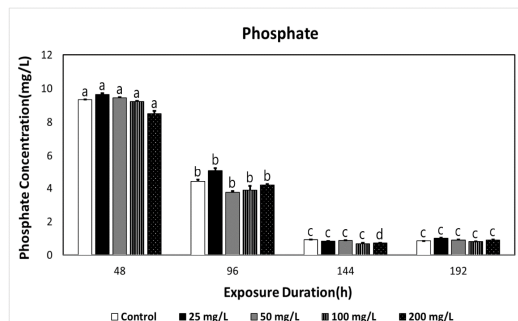


Fig. 14: Microalgae biomass of *C. vulgaris* in the presence of the same concentration of phosphate and microplastic. Lowercase letters indicate significant differences between groups ($p \leq 0.05$). The white, black, gray, striped, and dotted charts indicate nanoplastic

concentrations of 0, 50, 25, 100 and 200 mg/liter, respectively.

Discussion

Due to the widespread distribution of plastic particles at the nanoscale and their substantial impact on organisms, mainly marine organisms such as microalgae, it was found that the growth of *C. vulgaris* is strongly influenced by plastic nanomaterials and causes inhibition¹⁹. The size-dependent toxicity of polystyrene NPs coated with amine functional groups (PS-NH₂) investigated on biomass, photosynthetic pigments, and morphology of *C. vulgaris* microalgae. PS-NH₂-90 and PS-NH₂-200 can reduce algal biomass and chlorophyll in size-dependent treatments, whereas this trend was not observed for PS-NH₂-300. In a comprehensive survey, the effect of different polystyrene particle sizes (20, 50, 500 nm) on *C. vulgaris* at increasing intervals was investigated, and the percentage of viable cells and the chlorophyll concentration after exposure to polystyrene particles showed a significant difference²⁰. Various studies have reported that amino groups on the surface of NPs play an essential role in determining toxicity. Hence the uptake of PS-NH₂ in microalgae is dose-dependent (Toxicity increases with increasing concentration)^{21,22}. Another one of the main approaches in toxicity analyses is the estimation of cell viability indicating cellular reaction to a toxicant our cell viability results showed the importance of size in the toxicity effect. Likewise, in an enzymatic study with increasing nanoplastic size, the amount of enzymes increased in all assays performed except for the GSH because of production of reactive oxygen species (ROS) after exposure to polystyrene particles. Accordingly, based on previous studies, can be emphasized that the damage of the cell membrane and then cell death has occurred due to the small size of nanoplastic (PS-NH₂-90)^{15,20,23-26}. The reason for the increase amount sulfhydryl protein can be the cell membrane damage and finally the death of the algae cell in treatment PS-NH₂-90. Various studies have shown that nanoparticles bind highly to the lipid bilayers of cell membranes which causes the cell membranes damage and increase of protein, lipid, and thiol peptides^{27, 28}. The other pathway autooxidation of cell membrane lipids may also occur due to reactive oxygen species. This pathway prevents the oxidation of lipids and damage to them by activating the enzymatic antioxidant system such as glutathione -S-transferase (GST) and glutathione reductase and non-enzymatic factors such as glutathione. According to further studies, it seems that this pathway is activated in *C. vulgaris* when faced with PS-NH₂-200 and PS-NH₂-300^{29,30}. Since *Chlorella* microalgae are single-celled, the entire organism can be affected by nanoparticles. However, nanoparticle damage to multicellular organisms occurs through skin contact or inhalation^{31,32}. The spherical structure of chlorella algae can reveal useful information about

its health. Structural changes of microalgae after exposure to NPs are good evidence for the toxicity of these particles. After microalgae are exposed to environmental pollutants such as microplastic particles, the algal cell membrane acts as the first line of defense, because microplastics can penetrate them through the cell membrane^{33,34}. This state mainly depends on the size of the particles, the duration of exposure to microparticles, and the chemical properties of microplastics^{35,36}. Many mechanisms have been reported for the toxicity of nanoparticles, including the destruction of lipopolysaccharide molecules, inactivation of proteins and enzymes, production of reactive oxygen species, adhesion to cell membranes, inhibition of DNA synthesis, and increase in cell porosity³⁷. This is the reason why microalgae lose its bioremediation properties when faced with microplastics. The higher the concentration of microplastics, the greater its toxicity and the reduction of nitrate and phosphate in the treatment plant and biomass, which is very important from an economic point of view. To further evaluate the toxicity of PS-NH₂-90, PS-NH₂-200, and PS-NH₂-300 in *Chlorella* algae, the content of chlorophyll in the algae was also measured after 72 hours. The statistical results of chlorophyll a were similar to the statistical results of biomass. In other words, a statistically significant difference was found between the chlorophyll of the control group and the environments treated with different concentrations of PS-NH₂-90 and PS-NH₂-200 at the investigated times ($p < 0.05$). However, no statistically significant difference was observed for PS-NH₂-300. According to these interpretations, a direct relationship between algal biomass and chlorophyll content was observed, indicating that algal growth can be reduced by reducing chlorophyll content³⁷⁻³⁹.

Conclusions

Although the use of plastic materials is constantly increasing due to their cheapness, plastic waste is recognized as a severe threat to aquatic life. Plastics are fragmented into smaller particles (e.g., micro/nanoparticles) due to biodegradation, weathering, and degradation. In addition, human activities can deliberately release NPs into the environment. Through this study, the size-dependent toxicity of polystyrene NPs on biomass, the activity of enzymes such as superoxide dismutase (SOD), catalase (CAT), glutathione S-transferase (GST), and reduced glutathione concentration (GSH), carbonyl protein and the sulfhydryl protein and the level of antioxidant activity (with the DPPH reagent) were examined of the alga *C. vulgaris*. After exposure of *C. vulgaris* to PS-NH₂, abnormalities such as increased algal accumulation and decreased algal density were observed, and the size of the algae was also affected. To gain a deeper understanding of the response of microalgae to PS-NH₂

contamination, we recommend PS-NH₂ interaction with algae due to PS-NH₂ adhesion to algal cell surfaces. In all assays, the size of 90 nm showed the highest toxicity, which means that as the size of the nanoplastic decreases, its toxicity will increase. Then the toxicity effect of 90 nm NPs with a concentration of 200 mg/L on the microalgae *C. vulgaris* (with a concentration of 25000 Cells/mL) with the aim of bioremediation of nitrate (with a concentration of 50 mg/L) and phosphate (with a concentration of 6 mg/L) were investigated.

Acknowledgments

The authors gratefully acknowledge Alzahra University and Iran National Science Foundation (INSF) for their financial support.

Conflict of interest

The authors declare that there are no potential conflicts of interest in the present work.

Funding Sources

This work is part of a Ph.D. thesis supported financially by Alzahra University and Iran National Science Foundation (INSF).

References

1. Tunali, M.; Uzoefuna, EN.; Tunali, MM.; Yenigun, O. *Sci Total Environ.*, **2020**, *743*, 140479. doi: 10.1016/j.scitotenv.2020.140479.
2. Ho, BT.; Roberts, TK.; Lucas, S. *Crit Rev Biotechnol.*, **2018**, *38*, 308. doi: 10.1080/07388551.2017.1355293.
3. Kumar, M.; Chen, H.; Sarsaiya, S.; Qin, S.; Liu, H.; Awasthi, MK.; Kumar, S.; Singh, L.; Zhang, Z.; Bolan, NS.; Pandey, A.; Varjani, S.J.; Taherzadeh, Md. *J Hazard Mater.*, **2021**, *409*, 124967. doi: 10.1016/j.jhazmat.2020.124967.
4. Ng, EL.; Huerta Lwanga, E.; Eldridge, SM.; Johnston, P.; Hu, HW.; Geissen, V.; Chen, D. *Sci Total Environ.*, **2018**, *627*, 1377. doi: 10.1016/j.scitotenv.2018.01.341.
5. Bergami, E.; Pugnolini, S.; Vannuccini, ML.; Manfra, L.; Faleri, C.; Savorelli, F.; Dawson, KA. *Aquat Toxicol.*, **2017**, *189*, 159. doi: 10.1016/j.aquatox.2017.06.008.
6. Hanachi, P.; Karbalaeei, S.; Yu, S. *Environ Sci Pollut Res Int.*, **2021**, *28*, 64908. doi: 10.1007/s11356-021-15536-4.
7. Yee, MS.; Hii, LW.; Looi, CK.; Lim, WM.; Wong, SF.; Kok, YY.; Tan, BK.; Wong, CY.; Leong, CO. *Nanomaterials (Basel)*, **2021**, *11(2)*, 496. doi: 10.3390/nano11020496.
8. Goshtasbi, H.; Atazadeh, E.; Fathi, M.; Movafeghi, A. *Environ Sci Pollut Res Int.*, **2022**, *29*, 18805. doi: 10.1007/s11356-021-17057-6.

9. Oukarroum, A.; Bras, S.; Perreault, F.; Popovic, R. *Ecotoxicol Environ Saf.*, **2012**, *78*, 80. doi: 10.1016/j.ecoenv.2011.11.012.
10. Khoshnamvand, M.; Hanachi, P.; Ashtiani, S.; Walker, TR. *Chemosphere*, **2021**, *280*, 130725. doi: 10.1016/j.chemosphere.2021.130725.
11. Beauchamp, C.; Fridovich, I. *Anal Biochem.*, **1971**, *44*, 276. doi: 10.1016/0003-2697(71)90370-8.
12. Aebi, H. *Methods in Enzymology*: Academic Press; **1984**, *105*, 121.
13. Habig, WH.; Jakoby, WB. *Methods Enzymol.*, **1981**, *77*, 398. doi: 10.1016/s0076-6879(81)77053-8.
14. Beutler, E.; Duron, O.; Kelly, BM. *J Lab Clin Med.*, **1963**, *61*, 882.
15. Leroueil, PR.; Berry, SA.; Duthie, K.; Han, G.; Rotello, VM.; McNerny, DQ.; Baker, JR.; Orr, BG.; Holl, MM. *Nano Lett.*, **2008**, *8*, 420. doi: 10.1021/nl0722929.
16. Habeeb, AF. *Methods Enzymol.*, **1972**, *25*, 457. doi: 10.1016/s0076-6879(72)25041-8.
17. Shimada, K.; Fujikawa, K.; Yahara, K.; Nakamura, T. *Journal of agricultural and food chemistry*, **1992**, *40*, 945. doi: 10.1021/jf00018a005.
18. Clesceri, LS.; Greenberg, A.E.; Eaton, A.D. Standard Methods for the Examination of Water and Wastewater. 20th Edition, *American public health association*, Washington DC. **1998**; 9.
19. Bameri, T.; Naji, A.; Akbarzadeh, A. *Journal of Aquatic Ecology*, **2020**, *10*, 52.
20. Hazeem, LJ.; Yesilay, G.; Bououdina, M.; Perna, S.; Cetin, D.; Suludere, Z.; Barras, A.; Boukherroub, R. *Mar Pollut Bull.*, **2020**, *156*, 111278. doi: 10.1016/j.marpolbul.2020.111278.
21. Bhattacharya, P.; Lin, S.; Turner, JP.; Ke, PC. *The journal of physical chemistry C*, **2010**, *114*, 16556.
22. Li, T.; Cao, X.; Zhao, R.; Cui, Z. *Frontiers of Environmental Science & Engineering*, **2023**, *17*, 43.
23. Bexiga, MG.; Varela, JA.; Wang, F.; Fenaroli, F.; Salvati, A.; Lynch, I.; Lynch, I.; Simpson, JC.; Dawson, KA. *Nanotoxicology*, **2011**, *5*, 557. doi: 10.3109/17435390.2010.539713.
24. Wang, F.; Bexiga, MG.; Anguissola, S.; Boya, P.; Simpson, JC.; Salvati, A.; Dawson, KA. *Nanoscale*, **2013**, *5*, 10868. doi: 10.1039/c3nr03249c.
25. Van Lehn, RC.; Alexander-Katz, A. *Soft Matter*, **2011**, *7*, 11392.
26. Lin, J.; Alexander-Katz, A. *ACS nano*, **2013**, *7*, 10799.
27. Mahana, A.; Guliy, OI.; Mehta, SK. *Ecotoxicol Environ Saf.*, **2021**, *208*, 111662. doi: 10.1016/j.ecoenv.2020.111662.
28. Rezayian, M.; Niknam, V.; Ebrahimzadeh, H. *Toxicol Rep.*, **2019**, *6*, 1309. doi: 10.1016/j.toxrep.2019.10.001.
29. Karuppanapandian, T.; Moon, J-C.; Kim, C.; Manoharan, K.; Kim, W. *Australian Journal of Crop Science*, **2011**, *5*, 709-25.
30. Madhu, Kaur, A.; Tyagi, S.; Shumayla; Singh, K.; Upadhyay, SK. *Plant Cell Rep.*, **2022**, *41*, 639. doi: 10.1007/s00299-021-02717-1.
31. Khoshnamvand, M.; Ashtiani, S.; Huo, C.; Saeb, SP.; Liu, J. *Journal of Molecular Structure*, **2019**, *1179*, 749.
32. Moreno-Garrido, I.; Pérez, S.; Blasco, J. *Mar Environ Res.*, **2015**, *111*, 60. doi: 10.1016/j.marenvres.2015.05.008.
33. Cole, M.; Lindeque, P.; Fileman, E.; Halsband, C.; Goodhead, R.; Moger, J.; Galloway, TS. *Environ Sci Technol.*, **2013**, *47*, 6646. doi: 10.1021/es400663f.
34. Wang, S.; Liu, M.; Wang, J.; Huang, J.; Wang, J. *Mar Pollut Bull.*, **2020**, *158*, 111403. doi: 10.1016/j.marpolbul.2020.111403.
35. Shen, M.; Zhang, Y.; Zhu, Y.; Song, B.; Zeng, G.; Hu, D.; Wen, X.; Ren, X. *Environ Pollut.*, **2019**, *252*, 511. doi: 10.1016/j.envpol.2019.05.102.
36. Natarajan, L.; Omer, S.; Jetly, N.; Jenifer, MA.; Chandrasekaran, N.; Suraishkumar, GK.; Mukherjee, A. *Environ Res.*, **2020**, *188*, 109842. doi: 10.1016/j.envres.2020.109842.
37. Xiang, L.; Fang, J.; Cheng, H. *Environ Monit Assess.*, **2018**, *190*, 667. doi: 10.1007/s10661-018-7022-7.
38. Fadare, OO.; Wan, B.; Guo, L-H.; Xin, Y.; Qin, W.; Yang, Y. *Environmental Science: Nano*, **2019**, *6*, 1466.
39. Hazeem, LJ.; Yesilay, G.; Bououdina, M.; Perna, S.; Cetin, D.; Suludere, Z.; Barras, A.; Boukherroub, R. *Marine Pollution Bulletin*, **2020**, *156*, 111278.